J|A|C|S ARTICLES

Published on Web 10/29/2009

A Preliminary Survey of the Peptoid Folding Landscape

Glenn L. Butterfoss,*,† P. Douglas Renfrew,‡ Brian Kuhlman,‡ Kent Kirshenbaum,*,§ and Richard Bonneau*,†,||

Center for Genomics and Systems Biology, New York University, New York, New York 10003, Department of Biochemistry and Biophysics, University of North Carolina at Chapel Hill, Chapel Hill, North Carolina 27599, Department of Chemistry, New York University, New York, New York 10003, and Department of Computer Science, Courant Institute for Mathematical Sciences, New York, New York 10003

Received June 26, 2009; E-mail: gb77@nyu.edu; kent@nyu.edu; bonneau@nyu.edu

Abstract: We present an analysis of the conformational preferences of N-substituted glycine peptoid oligomers. We survey the backbone conformations observed in experimentally determined peptoid structures and provide a comparison with high-level quantum mechanics calculations of short peptoid oligomers. The dominant sources of structural variation derive from: side-chain dependent cis/trans isomerization of backbone amide bonds, side chain stereochemistry, and flexibility in the psi dihedral angle. We find good agreement between the clustering of experimentally determined peptoid torsion angles and local torsional minima predicted by theory for a disarcosine model. The calculations describe a well-defined conformational map featuring distinct energy minima. The general features of the peptoid backbone conformational landscape are consistent across a range of N-alkyl glycine side chains. Alteration of side chain types, however, creates subtle but potentially significant variations in local folding propensities. We identify a limited number of low energy local conformations, which may be preferentially favored by incorporation of particular monomer units. Greater variation in backbone dihedral angles are accessible in peptoids featuring trans amide bond geometries. These results confirm that computational approaches can play a valuable role in guiding the design of complex peptoid architectures and may lead to strategies for introducing constraints that select among a limited number of low energy local conformations.

Introduction

Peptoids are a class of peptidomimetic oligomers composed of N-substituted glycine units. The conformational properties and biomedical applications of peptoids have been the focus of considerable research in recent years, along with several other examples of "foldamer" compounds.[1−4] Notably, peptoids offer several attractive characteristics relative to peptides. Among these is a facile "submonomer" synthesis protocol that allows a vast number of primary amines to be used as synthons, enabling the introduction of diverse side chain functionalities. Peptoids exhibit broad resiliency to hydrolytic degradation by proteases. Despite their inability to form hydrogen bond networks, peptoids are known to adopt stable three-dimensional structures, which often localize in backbone conformational spaces not readily accessible to peptides.[5−7] For example, the cis and trans amide bond geometries of peptoids are generally iso-energetic, allowing peptoids to form poly proline I type helices featuring repeating cis amide bonds that are rarely observed in peptides. The backbone structural preferences in peptoids are predominantly driven by local interactions, including steric, stereoelectronic and bond-resonance effects.[8−10] These structural features, along with the inherent chemical diversity accessible via peptoid synthesis, provide a platform that is highly amenable for the *de novo* design of folded macromolecules.[11] In this work, we focus on enhancing our understanding of the local structural propensities of peptoids, using both experimental data and quantum mechanics simulations. These advances are an important step toward developing sequence-structure relationships suitable for designing more complex peptoid architectures.

† Center for Genomics and Systems Biology, New York University.
‡ University of North Carolina at Chapel Hill.
§ Department of Chemistry, New York University.
|| Courant Institute for Mathematical Sciences.

(1) Zuckermann, R. N.; Kodadek, T. *Curr. Opin. Mol. Ther.* **2009**, *11*, 299–307.
(2) Goodman, C. M.; Choi, S.; Shandler, S.; DeGrado, W. F. *Nat. Chem. Biol.* **2007**, *3*, 252–262.
(3) Fowler, S. A.; Blackwell, H. E. *Org. Biomol. Chem.* **2009**, *7*, 1508–1524.
(4) Yoo, B.; Kirshenbaum, K. *Curr. Opin. Chem. Biol.* 2008.
(5) Armand, P.; Kirshenbaum, K.; Goldsmith, R. A.; Farr-Jones, S.; Barron, A. E.; Truong, K. T.; Dill, K. A.; Mierke, D. F.; Cohen, F. E.; Zuckermann, R. N.; Bradley, E. K. *Proc. Natl. Acad. Sci. U.S.A.* **1998**, *95*, 4309–4314.
(6) Huang, K.; Wu, C. W.; Sanborn, T. J.; Patch, J. A.; Kirshenbaum, K.; Zuckermann, R. N.; Barron, A. E.; Radhakrishnan, I. *J. Am. Chem. Soc.* **2006**, *128*, 1733–1738.
(7) Wu, C. W.; Kirshenbaum, K.; Sanborn, T. J.; Patch, J. A.; Huang, K.; Dill, K. A.; Zuckermann, R. N.; Barron, A. E. *J. Am. Chem. Soc.* **2003**, *125*, 13525–13530.
(8) Gorske, B. C.; Bastian, B. L.; Geske, G. D.; Blackwell, H. E. *J. Am. Chem. Soc.* **2007**, *129*, 8928–8929.
(9) Choudhary, A.; Gandla, D.; Krow, G. R.; Raines, R. T. *J. Am. Chem. Soc.* **2009**, *131*, 7244–7246.
(10) Shah, N. H.; Butterfoss, G. L.; Nguyen, K.; Yoo, B.; Bonneau, R.; Rabenstein, D. L.; Kirshenbaum, K. *J. Am. Chem. Soc.* **2008**, *130*, 16622–16632.
(11) Armand, P.; Kirshenbaum, K.; Falicov, A.; Dunbrack, R. L., Jr.; Dill, K. A.; Zuckermann, R. N.; Cohen, F. E. *Fold Des.* **1997**, *2*, 369–375.

 10.1021/ja905267k CCC: $40.75

Table 1. Experimental Structures Used in This Study

sequence[a]	molecule[b]	experimental method	chain length
cyclo-(Sar)$_8$[c]	8	X-ray	8
cyclo-(Npm-Nme)$_3$[d]	9	X-ray	6
cyclo-(Npm-Nme)$_4$[d]	10	X-ray	8
cyclo-(Nbe)$_4$[e]	11	X-ray	4
cyclo-(Nbe)$_6$[e]	12	X-ray	6
(Nrch)$_5$[f]	13	X-ray	5
cyclo-(Nspe)$_6$[g]	14	X-ray	6
(Nspe)$_9$[h]	15	NMR	9
cyclo-(Nspe-Nph-Nspe)$_2$[i]	16	X-ray	6
Nnp-Nph[i]	17	X-ray	2

[a] residue types: Sar, sarcosine; Npm, *N*-(phenylmethyl)glycine; Nme, *N*-(methoxyethyl)glycine; Nbe, *N*-(benzyloxyethyl)glycine; Nrch, (*R*)-*N*-(1-cyclohexylethyl)glycine; Nspe, (*S*)-*N*-(1-phenylethyl)glycine; Nnp, *N*-(2-nitro-3-hydroxyl phenyl)glycine; Nph, *N*-(phenyl)glycine. [b] See Scheme 3. [c] Reference 15. [d] Reference 14. [e] Reference 16. [f] Reference 7. [g] Reference 23. [h] Reference 6. [i] Reference 10.

One relative advantage in studying the folding characteristics of proteins is access to a large database of known protein structures. Thus, protein-folding and modeling studies have an extensive set of examples in the Protein Data Bank that enable the development of effective energy functions and search algorithms.[12,13] Unfortunately, much less structural data is available for peptoids than for peptide and protein systems. However, several high-resolution peptoid structures have been solved in recent years. Individual structures are listed in Table 1. Notable structures include a 9-mer "threaded loop" fold and a helix resembling the polyproline type I structure.[6,7] Additionally, a number of cyclized peptoid crystal structures have been determined to form hairpin turns including a variety of lengths and cis/trans omega bond distributions.[14−16] The fact that peptoids are able to form a variety of secondary structural elements, including helices and hairpin turns, suggests a range of possible conformations that will allow the generation of functional folds.[17]

In the absence of a large data set of high-resolution peptoid structures, the conformational and energetic consequences of various amide nitrogen substituents may be thoroughly investigated with theoretical models. In this work, we use a hybrid approach in which overall conformational landscapes are evaluated using quantum mechanics calculations and subsequently validated by our survey of recent peptoid experimental structures.

Previous studies have sought to characterize the peptoid backbone conformational landscape. Simon et al. calculated Ramachandran-type plots for several dipeptoid models and suggested the dihedral angles (ϕ, ψ) = (−120°, 90°) and (120°, −90°) as the global minima for disarcosine (see Scheme 1 for angle definitions).[18,19] However, this work relied on molecular mechanics models that were not parametrized for peptoids. Moehle and Hofmann used *ab initio* quantum mechanics to model a disarcosine analogue and found unique low energy conformations that do not correspond with those observed for peptides.[20] Stable points on the energy surface were identified at six conformations (with approximate (ϕ, ψ) values): cis and trans $C_{7\beta}$ (−130°, 80°), cis and trans α_D (75°, 180°), and higher energy minima at cis and trans α (−60°, −40°).[21] Additional theoretical studies have focused on identifying the propensities of peptoids to form helices. Armand et al. used molecular mechanics and semiempirical models to predict accurately that peptoid oligomers bearing bulky chiral (*S*)-*N*-(1-phenylethyl) side chains would adopt a polyproline type I helical conformation, in agreement with subsequent experimental findings.[11] The predicted backbone conformation, cis (−75°, 170°), is essentially the mirror image of the cis α_D conformation mentioned above. Baldauf et al. also explored helical propensities of sacrosine hexamers with quantum models and identified polyproline type I and II type helices (oligomers of cis and trans of cis and trans α_D, respectively) as the most stable helices.[22] Our previous work has shown agreement between quantum models and the trans amide of N-aryl peptoids, and suggested that they may form polyproline type II helices.[10] Combined, these studies suggest that the backbone conformational propensities evident at the local level may be readily translated into the conformations of larger oligomer chains.

We now have both the computational resources and experimental data to expand on these studies, enabling us to construct a complete landscape of peptoid backbone energies and to determine how well local energetics predict the observed conformations and atomic-resolution details of peptoid structures. We find that the experimental distributions of ω, ϕ, and ψ torsions fall within low energy contours predicted by theory, and that dependencies between ω vs ϕ, and also ω vs ψ, might be important parameters for evaluating and predicting peptoid structures. Ramachandran-type analysis reveals that experimental structures cluster around predicted energy minima corresponding to the trans $C_{7\beta}$, trans α_D, and cis α_D conformations. Further-

Scheme 1. (A) Molecule **1** with Assignment of Backbone Torsions[a] and (B) Peptoid χ_1 Angle[b]

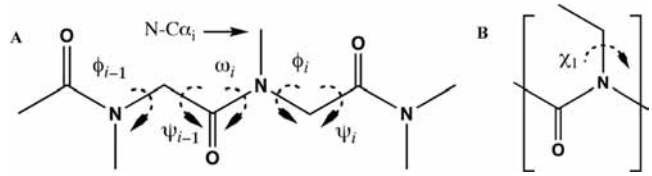

[a] N−Cα atom for residue *i* is identified by the solid arrow. [b] Measured here from the amide carbon of the preceding residue.

(12) Rohl, C. A.; Strauss, C. E.; Misura, K. M.; Baker, D. *Methods Enzymol.* **2004**, *383*, 66–93.
(13) Berman, H. M.; Westbrook, J.; Feng, Z.; Gilliland, G.; Bhat, T. N.; Weissig, H.; Shindyalov, I. N.; Bourne, P. E. *Nucleic Acids Res.* **2000**, *28*, 235–242.
(14) Shin, S. B.; Yoo, B.; Todaro, L. J.; Kirshenbaum, K. *J. Am. Chem. Soc.* **2007**, *129*, 3218–3225.
(15) Tiltlestad, K.; Groth, P.; Dale, J.; Ali, M. Y. *Chem. Commun.* **1973**, 346–347.
(16) Maulucci, N.; Izzo, I.; Bifulco, G.; Aliberti, A.; De Cola, C.; Comegna, D.; Gaeta, C.; Napolitano, A.; Pizza, C.; Tedesco, C.; Flot, D.; De Riccardis, F. *Chem. Commun.* **2008**, 3927–3929.
(17) Maayan, G.; Ward, M. D.; Kirshenbaum, K. *Proc. Natl. Acad. Sci. U.S.A.* **2009**, *106*, 13679–13684.
(18) Simon, R. J.; Kania, R. S.; Zuckermann, R. N.; Huebner, V. D.; Jewell, D. A.; Banville, S.; Ng, S.; Wang, L.; Rosenberg, S.; Marlowe, C. K. *Proc. Natl. Acad. Sci. U.S.A.* **1992**, *89*, 9367–9371.
(19) Ramachandran, G. N.; Ramakrishnan, C.; Sasisekharan, V. *J. Mol. Biol.* **1963**, *7*, 95–99.
(20) Moehle, K.; Hofmann, H. J. *Biopolymers* **1996**, *38*, 781–790.
(21) It is important to note that there is some disagreement between various papers in how to assign ω to a particular peptoid residue, in our work we follow the method of Moehle and Hofmann (see the methods section for rationale).
(22) Baldauf, C.; Gunther, R.; Hofmann, H. J. *Phys. Biol.* **2006**, *3*, S1–S9.
(23) Yoo, B. Kirshenbaum, K., *in preparation*.

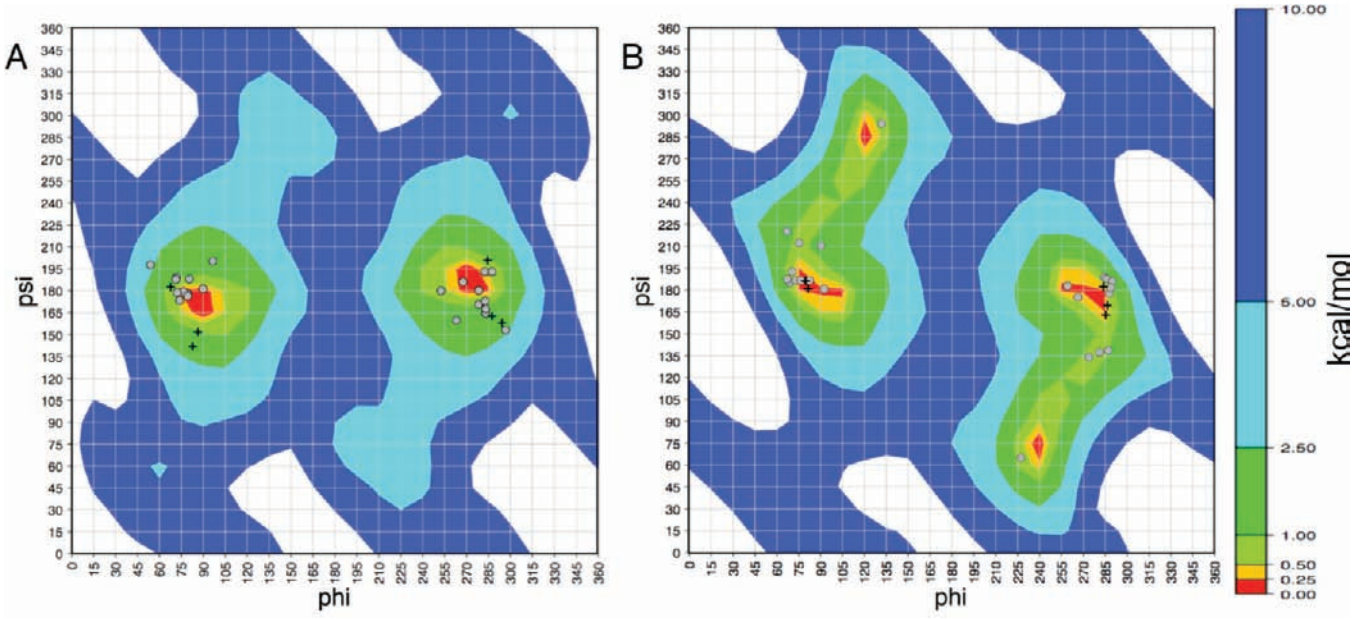

Figure 1. Ramachandran-type plots of residues in experimental peptoid structures overlaid on a B3LYP/6-31+1G(2d,p)// HF/6-31G* energy landscape (in kcal/mol) of molecule **1**. (A) ω is cis, (B) ω is trans. Points are residue conformations in cyclic (circles) and linear (crosses) peptoids. The zero energies are set to the lowest value in each plot. See Methods for details.

more, we show how variation in peptoid side chains may influence the favorability of the various local energy minima.

Results and Discussion

Experimental Data. Atomic resolution structural data on peptoids is still somewhat sparse. In this study, we used a data set of 10 high-resolution peptoid structures (9 determined by X-ray diffraction and 1 by solution NMR methods). Of the set, 7 are cyclic and 3 are linear (Table 1). This resulted in a data set of 55 (ϕ, ψ) pairs, 50 ω points, 50 (ω, ϕ) pairs, and 48 (ω, ψ) pairs (see Methods).

ϕ vs ψ Distributions of Peptoids. Ramachandran-type plots of (ϕ, ψ) distributions are an established method to interpret protein structure, as these torsions are the dominant degrees of freedom in peptide backbones. To better understand the local preferences of peptoid backbones along these dimensions, we screened the cis and trans amide Ramachandran energy surface of molecule **1**.[19] We chose this end-capped disarcosine compound as an appropriate model for intrinsic peptoid backbone behavior, as it contains a complete ω, ϕ, ψ series and a typical surrounding chemical environment representative of those present in longer peptoid oligomers. Figure 1 shows the predicted energy landscapes of molecule **1** in both cis (Figure 1A) and trans (Figure 1B) ω conformations overlaid with (ϕ, ψ) distributions of the experimental structures. Plots are from 0 to 360° rather than the traditional −180 to 180° to more clearly illustrate the peptoid-relevant minima. Unlike the Ramachandran plots for the canonical chiral nonglycine amino acids, the energy surface for the achiral peptoid **1** is center symmetric, i.e. the energy of a structure with a given (ϕ, ψ) will be identical to its mirror image with ($-\phi$, $-\psi$) (see methods for details).

Inspection of experimentally observed structures shows that for residues with cis ω (Figure 1A), the corresponding ϕ and ψ dihedral angles all cluster around center-symmetric positions at (±90°, 180°) (note: −90° = 270°). Peptoid conformations in the vicinity of (90°, 180°) have previously been termed α_D. Here, we use this designation for both center-symmetric conformations.[20] The (−90°, 180°) cis α_D conformation approximates the poly proline I helix rarely found in peptides. The calculated energy surface for the cis conformation of molecule **1** (ϕ, ψ) correspondingly has deep minima near (±90°, 180°). Moderate energy valleys ($2.5 < x < 5$ kcal/mol) extend to approximately (135°, 315°) and (225°, 45°) from the minima at (90°, 180°) and (−90°, 180°), respectively. However, no experimental conformations populate these valleys. All of the experimental points cluster within, or lie in close proximity to, the 2.5 kcal/mol contour.

Experimentally determined structures feature trans ω residues that also cluster around the trans α_D conformation (±90°, 180°), which agrees with our previous studies of trans N-aryl peptoids[10] (Figure 1B). Trans α_D (−90°, 180°) is similar to the conformation of the poly proline II helix. In both the cis and trans Ramachandran plots, the experimental structures and predicted landscapes are tightly clustered around $\phi = \pm 90°$, suggesting that ϕ has limited flexibility in peptoids. However, the experimental structures show, and our calculations predict, somewhat greater variation in ψ when ω is trans; whereas cis has one main center symmetric minimum, the trans surface has two local minima around (±90°, 180°) and {(−120°, 75°), (120°, −75°)}, the latter minima pair corresponds to the previously identified trans $C_{7\beta}$ conformation.[20] An energetically accessible valley runs between trans α_D and trans $C_{7\beta}$ (~1 kcal/mol above the lowest minima). This valley is populated by six experimental conformations with ψ at approximately ±135°. All of the experimental points corresponding to trans amide bonds ($\omega \approx 180°$) fall within or near the 1.0 kcal/mol contour above the trans minimum.

Although the trans $C_{7\beta}$ is nearly isoenergetic with the trans α_D conformation at this level of theory, $C_{7\beta}$ is only represented in two residues from a single structure. Both are in the tight turns of a cyclic tetramer (molecule **11**, Figure 2).[16] Hence the trans $C_{7\beta}$ conformation, when followed by a cis ω angle, allows for a sharp backbone hairpin, and, despite being a small macrocycle, the (ϕ, ψ) pairs in this tetramer are all near predicted local energy minima. The trans $C_{7\beta}$ conformation may be precluded by interactions with neighboring residues such as a

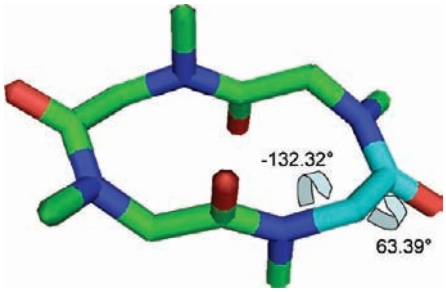

Figure 2. Backbone structure of molecule **11** showing a $C_{7\beta}$ conformation in cyan (ϕ, ψ) = (−132°, 63°). For clarity, only N−Cα side chain atoms are shown.

steric clash between the backbone oxygen of residue *i* and a large rigid side chain of residue *i*+1. When an analogue of molecule **1** with a trans N-aryl side chain at *i*+1 is minimized at the HF/6-31G* level staring from a (120°, −75°) $C_{7\beta}$ conformation, ψ_i relaxes 25° to (129.16°, −102.16°) (see Supporting Information Figure S3). Moreover, the trans $C_{7\beta}$ minima are not observed in our previous calculations with *N*-phenyl-glycine dipeptoid analogue, possibly due to steric clashes between the side chain and the Cα methylene or the carbonyl oxygen.[10]

A comparison of the B3LYP/6-31G*//HF/6-31G* and MP2/6-31G*//HF/6-31G* potential energy landscapes is given in the Supporting Information (Figure S2). The two model chemistries differ in their major deficiencies with regards to this system, that is, poor representation of dispersion forces in density functional theory, and basis set super position effects overfavoring more compact geometries for MP2.[24,25] Strong correlation between the potential energy surfaces, particularly in the regions surrounding the local minima, suggest that neither of form of error is leading to significant perturbations within the accessible regions of the cis or trans amide landscapes. Given this agreement, we focus on predictions with density functional methods below, due, in part, to the weaker basis set dependence, greater computational efficiency, and for consistency with previous work.[10]

When these local minima conformations are allowed to relax freely without constraints at the HF/6-31G* level, strikingly, the optimized omega torsions have large deviations from planarity in the cis and trans α_D conformations (Table 2). The Supporting Information provides the structures of the minimized conformations and a detailed analysis of their relative energies (Tables S1 and S2).

Amide Nonplanarity in Peptoids. The extent to which amide bond systems are planar in proteins has been a subject of considerable research.[26−32] Notably, Corey and Pauling cautioned that a "structure in which the atoms of the amide group are not approximately coplanar should be regarded with skepticism until its relatively unstable configuration has been adequately confirmed."[33] MacArthur and Thornton found that the structures reported for small linear and cyclic peptides exhibited more nonplanarity than full protein structures and suggested this may be due to overfitting of amide planarity during refinement of crystallographic data.[26] Accurate potentials for amide nonplanarity may be an important consideration for peptoid modeling and refinement, as local interactions generated by bulky side chains bonded directly to nitrogen may perturb the amide system.

Scheme 2. Peptoid Models Evaluated

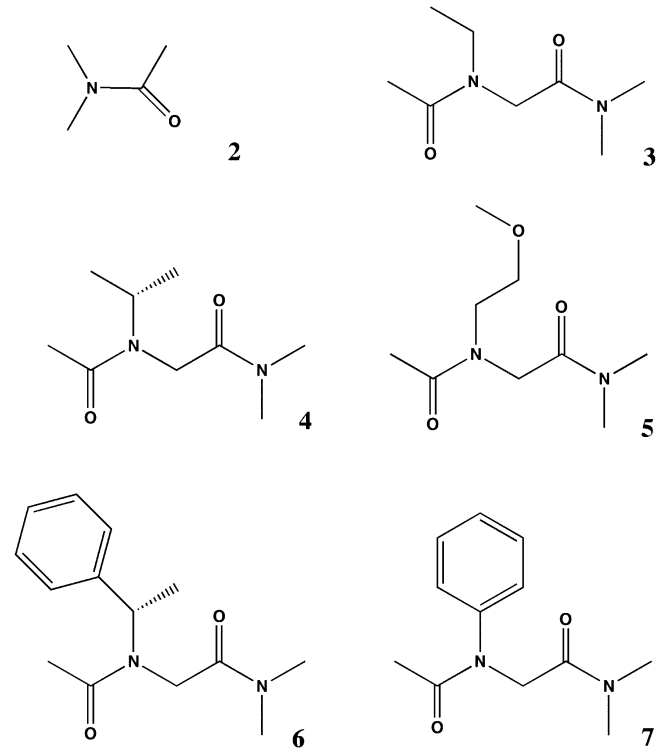

We estimated a basic potential for the ω torsion in peptoids with *N*,*N*-dimethylacetamide (molecule **2**, Scheme 2), a simple model of a peptoid amide bond. We compared the predicted Boltzmann distribution of ω in molecule **2** at 300K with ω values from the experimental X-ray structures (Figure 3). Both experimental and theoretical methods show a slightly broader distribution at half width for the cis conformer relative to trans ω, although this broadening is less pronounced in the crystallographic data. The theoretical cis and trans distributions are not identical because the N-dimethyl group does not move as a rigid plane and the methyl in the cis conformer is predicted to have more freedom than the trans. However, the experimental data set here consists primarily of cyclized compounds, so one must be careful not to overinterpret these results, as some of the deviation may be due to constraints arising from macrocycle closure. A more detailed analysis of nonplanarity using Dunitz parameters is given in the Supporting Information.[34]

Peptoids exhibit significant interconversion between cis and trans amide bonds and substantial deviations from amide planarity.[10,35] Thus, freedom in ω is an important characteristic

(24) Holroyd, L. F.; van Mourik, T. *Chem. Phys. Lett.* **2007**, *442*, 42–46.
(25) van Mourik, T.; Karamertzanis, P. G.; Price, S. L. *J. Phys. Chem. A* **2006**, *110*, 8–12.
(26) MacArthur, M. W.; Thornton, J. M. *J. Mol. Biol.* **1996**, *264*, 1180–1195.
(27) Edison, A. S. *Nat. Struct. Biol.* **2001**, *8*, 201–202.
(28) Selvarengan, P.; Kolandaivel, P. *Bioorg. Chem.* **2005**, *33*, 253–263.
(29) Bednarova, L.; Malon, P.; Bour, P. *Chirality* **2007**, *19*, 775–786.
(30) Ramek, M.; Yu, C. H.; Sakon, J.; Schafer, L. *J. Phys. Chem. A* **2000**, *104*, 9636–9645.
(31) Pauling, L.; Corey, R. B.; Branson, H. R. *Proc. Natl. Acad. Sci. U.S.A.* **1951**, *37*, 205–211.
(32) Ramachandran, G. N. *Biopolymers* **1968**, *6*, 1494–1496.
(33) Corey, R. B.; Pauling, L. *Proc. R. Soc. Lond. B: Biol. Sci.* **1953**, *141*, 10–20.
(34) Winkler, F. K.; Dunitz, J. D. *J. Mol. Biol.* **1971**, *59*, 169–182.
(35) Sui, Q.; Borchardt, D.; Rabenstein, D. L. *J. Am. Chem. Soc.* **2007**, *129*, 12042–12048.

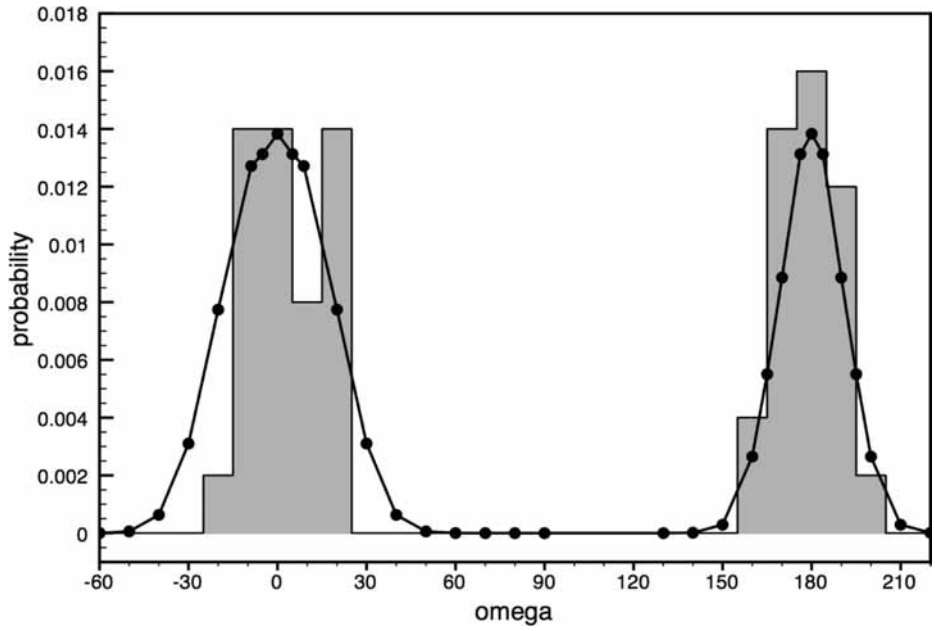

Figure 3. Comparison of ω torsion angle distributions in experimental peptoid structures and predicted probabilities for molecule **2**. Gray histogram is distribution from experimental X-ray structures. Filled circles represent a Boltzmann distribution for ω in molecule **2** based on B3LYP/6-311+G(2d,p)// HF/6-31G* energies and assuming a temperature of 300 K.

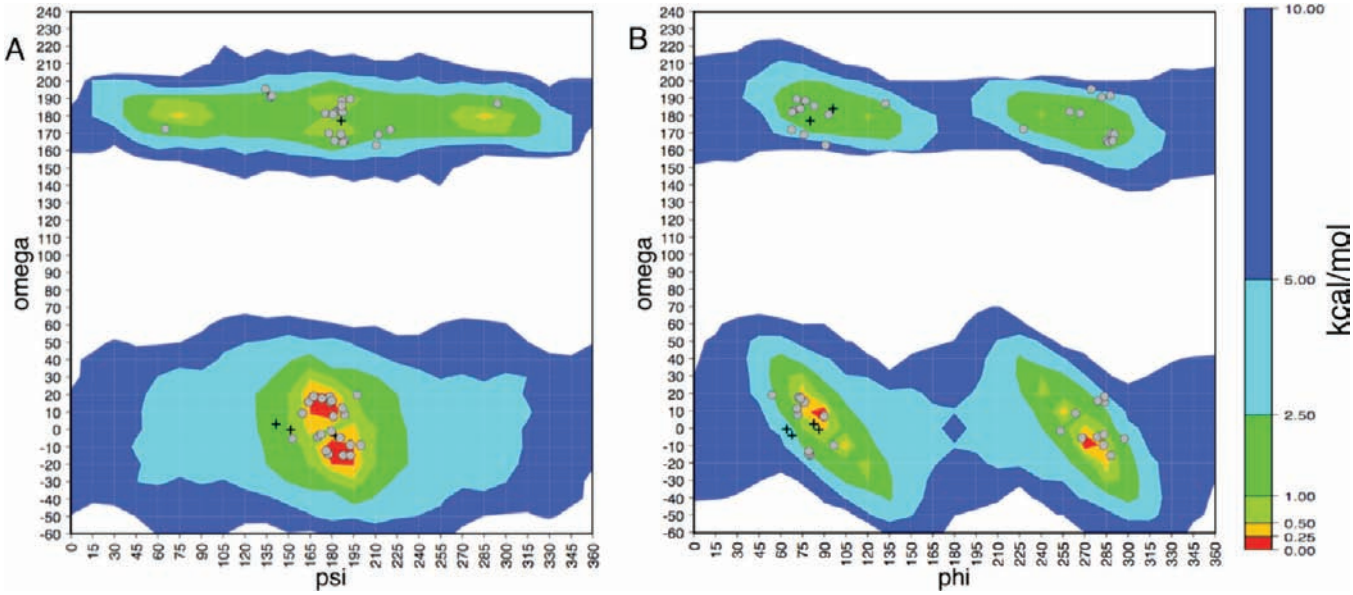

Figure 4. (A) ω vs ψ and (B) ω vs ϕ plots. Points are residue conformations in cyclic (circles) and linear (crosses) peptoid X-ray structures. Contours are energy landscapes calculated for molecule **1** at the B3LYP/6-31G*//HF/6-31G* level (in kcal/mol). See Methods for details.

of peptoid structural behavior and the standard Ramachandran-type plots discussed above may be insufficient representations for describing peotoids. To further understand peptoid ω deviations, we examined distributions of ϕ vs ω and ψ vs ω. We observed that the predicted energy surfaces of molecule **1** corresponded to the crystallographically determined conformations for ψ vs ω and ϕ vs ω (Figure 4 A and B. respectively). The minima evident in 4A are: cis α_D around (ψ, ω) (180°, 0°), trans α_D around (180°, 180°) and the two trans $C_{7\beta}$ minima at approximately (90°, 180°) and (300°, 180°). The cis and trans α_D experimental conformations cluster in accord with the energy surface. All experimental points fall near or within the 2.5 kcal/mol contour.

The relationship between ϕ and ω is similarly depicted in Figure 4B. The energy landscape shows four minima. The cis α_D conformations are represented by two wells roughly centered on two line segments with end-points at approximately (ϕ, ω) {(50°, 50°), (130°, −30°)} and {(230°, 30°), (310°, −50°)}. The experimentally determined values colocalize to these minima, indicating a strong dependence between ϕ and ω in cis peptoids. The trans α_D and $C_{7\beta}$ conformations form valleys centered on approximately (90°, 180°) and (270°, 180°). The energy contours suggest a weaker coupling between ϕ and ω in trans conformations. The distribution of the experimental points matches the shape defined by the energy contours of the minima.

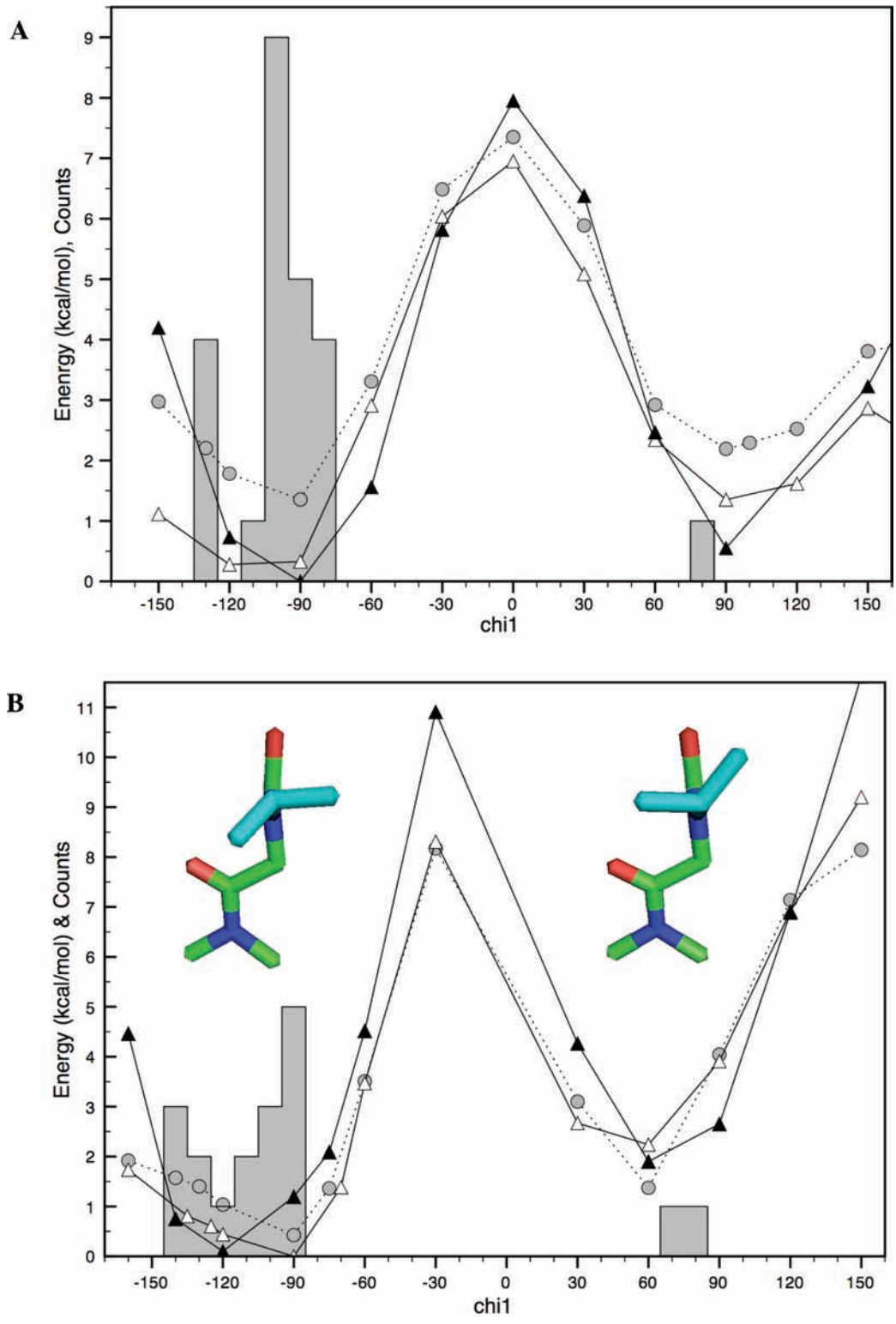

Figure 5. Histograms of distributions from peptoid crystal structures with energies for χ_1 rotations for molecules **3** (A) and **4** (B) at the B3LYP/6-311+G(2d,p)//HF/6-31G* level. For A the experimental set includes methylene N−Cα residues: *N*-(phenylmethyl)glycine, *N*-(methoxyethyl)glycine, and *N*-(benzyloxyethyl)glycine. For B the experimental residues are all (*S*)-*N*-(1-phenylethyl)glycine. Theoretical predictions are for 3 different backbone conformations cis α_D (ϕ, ψ) = (−90°, 180°) (circles), trans α_D (−90°, 180°) (open triangles), and trans $C_{7\beta}$ (−130°, 80°) (filled triangles). The experimental data in A were converted to ($-\phi$, $-\psi$, $-\chi_1$) if $\phi > 0$. Molecular structures in B show $\chi_1 = -90°$ (left) +90° (right) according to our convention.

Side Chains. We further investigated the energy preferences of peptoid χ_1 angles and the effects of side chain types on peptoid energy landscapes. Peptoid side chains can be segregated into three major classes with respect to the chemistry at N−Cα: N-aryl (molecule **7**), N−Cα-methylene (molecules **2**, **3**, and **5**), and N−Cα-branched (molecules **4** and **6**). We have previously investigated N-aryl side chains in detail, finding that χ_1 prefers ∼90° in a wide shallow energy well.[10] Here, we investigate N−Cα-methylene and N−Cα-branched side chains. First, we studied χ_1 preferences

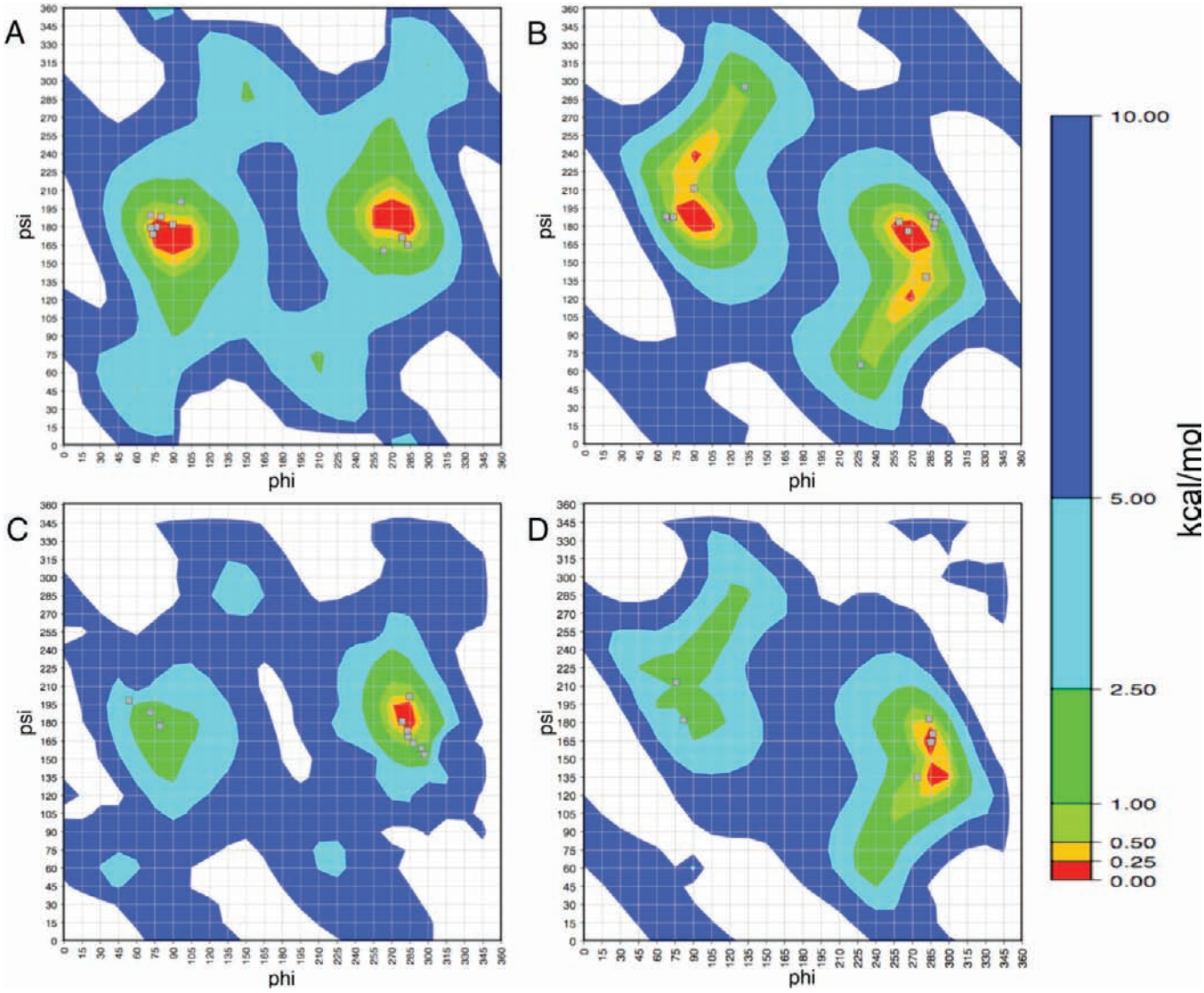

Figure 6. Comparison of Ramachandran-type energy surfaces of peptoids bearing achiral vs chiral side chains. Molecules **5** (A, B) and **6** (C, D) calculated at the B3LYP/6-311+G(2d,p)//HF/6-31G* level. For the left plots (A, C) ω is cis and for the right plots (B, D) ω is trans. Squares are corresponding experimental residues from crystal structures. For A and B, this includes methylene N−Cα residues: *N*-(phenylmethyl)glycine, *N*-(methoxyethyl)glycine, and *N*-(benzyloxyethyl)glycine. For C and D, the experimental residues are all (S)-*N*-(1-phenylethyl)glycine.

using molecules **3** and **4** as representatives of these two classes. For both molecules, we rotated around χ_1 while holding the backbone fixed at either cis α_D (−90°, 180°) trans α_D (−90°, 180°) or trans $C_{7\beta}$ (−130°, 80°). For the N−Cα-methylene model (molecule **3**) (Figure 5A), χ_1 shows two accessible rotameric states at roughly ±90° for all three backbone conformers. Additionally, for all three backbone conformers, −90° is slightly preferred to +90°. A comparison with the experimental data supports this prediction: experimental χ_1 values shows dominant localization around −90°. As this is an achiral system, the experimental χ_1 values were multiplied by −1 if ϕ was >0° so as to better match the backbone conformation of the model compound.

A similar analysis of the N−Cα-branched model (molecule **4**) shows predicted minima around χ_1 of approximately −90° and 60°, with a preference for the region around −90° in all three backbone conformers (Figure 5B).[36] The theoretical predictions and the experimental χ_1 conformations of (*S*)-*N*-(1-phenylethyl)glycine (Nspe) side chains show a preference for a rotamer in which both side chain methyl groups are projected toward the N-terminus. In the case of the N−Cα-branched conformations, the experimental data were not adjusted for center symmetry as above.

Side Chain Influence on ϕ and ψ Propensities. The experimentally determined ϕ and ψ dihedral angles plotted in Figure 1 include peptoids bearing a variety of side chains. As these conformational distributions agree well with predictions based on a disarcosine model, it is likely that the peptoid Ramachandran energy surface will be relatively consistent for a variety of side chains. To further investigate the influences of the side chain on backbone conformational preferences, we generated (ϕ, ψ) energy surfaces (Figure 6) for models of two side chains present in our experimental set, N-methoxyethyl (molecule **5**) and Nspe (molecule **6**). These represent both an N−Cα-methylene and an N−Cα-branched side chain. In general, the plots are quite consistent with energy landscapes observed for molecule **1** (Figure 6A and B). The trans $C_{7\beta}$ minima become

(36) We defined χ_1 as the torsion to the methyl group which corresponds to the phenyl group in the Nspe side chain.

less distinct for molecule **5** (Figure 6B) but the ~1 kcal/mol contour traces nearly the same shape as the sarcosine model for both cis and trans. The experimental points for N−Cα-methylene side chains all fall within or very close to the predicted 1 kcal/mol contour.

The energy surface for the Nspe side chain indicates much steeper energy gradients (Figure 6C and D) (implying more restricted freedom of motion). This finding is consistent with spectroscopic observations that bulky chiral side chains are structure-inducing elements in peptoid oligomers.[5,7] The region from the trans α_D minima toward the trans $C_{7\beta}$ conformation is not as favorable for molecule **6** relative to molecules **1** and **5**. The chiral side chain breaks the center symmetry and the backbone is predicted to prefer (−90°, 180°) to (90°, 180°) in both cis and trans conformers by over 1 kcal/mol. The experimental Nspe conformations tend to follow these chiral preferences, with 7 of the 11 cis residues (Figure 6C) and 4 out of 6 trans residues (Figure 6D) in the conformation with the lower predicted energy.

Conclusions

Peptoid Conformation. We have compared high-level quantum mechanics simulations of small molecule peptoid models with the set of available experimental structures of peptoid oligomers. We find close agreement between the theoretical predictions and the observed conformational preferences of peptoids, providing evidence that peptoid structural propensity is largely dictated by local energetics. Experimental distributions of ϕ vs ψ, ϕ vs ω, and ψ vs ω torsions all fall within a small set of low energy conformations predicted by theory. Experimental deviations of ω away from planarity are recapitulated by calculations with a sarcosine analogue and N,N-dimethylacetamide. We find that experimental and theoretical χ_1 distributions correspond to a 2-state rotamer model with predictable preferences for both N−Cα-methylene and N−Cα-branched side chains. We also show that bulky chiral side chains can be used to adjust the relative energies of various low energy peptoid backbone conformations.

The classical Ramachandran-type plot may not be as descriptive a representation of peptoid structure as it is for polypeptides. Amide bond isomerization is a dominant degree of freedom for the peptoid backbone and in our experimental data set, the ω torsion varies significantly from planarity (up to ~20° in both cis and trans).[19] The deviations are correlated with other backbone angles, in particular ϕ when ω is cis (Figure 4B). Freedom in ω is not accounted for in typical Ramachandran plots and future studies may find that ψ vs ω and ϕ vs ω plots are a more useful tool for depicting the local structural features of peptoid folds.

We have used a small experimental data set that largely consists of macrocycles for comparison, but we see no reason, *a priori*, why the observed behaviors would necessarily deviate in larger structures. This is in contrast to peptides and proteins, where hydrogen bonding interactions between noncontiguous residues can play an important role in defining backbone structure.

Implications for Rational Design. Peptoids appear to have a rather simple conformational map, in which the dominant sources of variability are: cis/trans ω isomerzation, side chain stereochemistry, and flexibility in ψ when the residue is in a trans ω conformation. This suggests that peptoids may be an attractive platform for rational foldamer design, provided sets of side chains or other constraints are developed to select among the limited low energy local conformations.[8]

Future Considerations. The potential energy surfaces were modeled in vaccuo without consideration of potential solvent effects. The preference of alanine containing peptides for the poly proline II conformations is known to be influenced by solvent —including changes as subtle as D_2O vs H_2O.[37,38] Additionally, the propensity of poly proline helices for the poly proline I PPI or poly proline II is quite sensitive to solvent and small chemical modifications, suggesting that the same may be true of the balance between the local minima in peptoids.[39−41] Indeed, previous studies and our own analysis of the local minima provided in the Supporting Information indicate that solvent can influence the relative energies.[20] As solvent effects are challenging to model accurately—and peptoids may be desired for use in a broad range of solvents—this is an important area for future investigation.

Our motivation, in addition to shedding light on local structural tendencies of peptoids, is to determine the degree to which we can rely on *ab initio* calculations to develop energy functions that can be used to design folded peptoids. Previous studies have shown the utility of using *ab initio* calculations to improve rotamer representations of protein side chains.[42,43] Thus, agreements between experimental structures and the predicted energy landscapes support the notion that accurate energy functions for peptoids may be based on *ab initio* calculations of small model compounds. The extent to which accurate modeling of complex amide deformations, such as pyramidalization, will be necessary for accurate prediction of peptoid structure remains an open question. In summary, our investigation supports the notion that peptoids are a predictable platform for developing the rational design of complex foldamer structures and functions.

Materials and Methods

Assigning Angles. The convention for assigning backbone torsions to an individual residue i in proteins is: ϕ and ψ are rotations about the bonds before and after Cα, respectively, and ω spans Cα of i to Cα of i+1. This system may be ill-suited to peptoids, as the side chain bonded to the nitrogen have may have significant influence on the cis/trans preferences of the amide bond between residues i−1 and i.[10] Thus, we follow the convention that ω of residue i is from Cα of i−1 to Cα of i (Scheme 1), which has been employed previously with peptoids.[20] In addition, we define the side chain torsion angle χ_1 as C(i−1)−N−(N−Cα)−(N−Cβ).

Experimental Structures. The set of experimental structures are reviewed in detail in the results section (Table 1, Scheme 3). Briefly, we used a set of 10 high-resolution structures (9 X-ray and 1 NMR).[6,7,10,14–16,23] Three of the structures are linear and 7 are macrocycles. The data set gave 55 experimental (ϕ, ψ) positions. To be conservative, we did not include the NMR structure in comparisons of ω distributions (Figures 3 and 4) due to greater uncertainty of the torsions.[6]

(37) Liu, Z.; Chen, K.; Ng, A.; Shi, Z.; Woody, R. W.; Kallenbach, N. R. *J. Am. Chem. Soc.* **2004**, *126*, 15141–15150.
(38) Chellgren, B. W.; Creamer, T. P. *J. Am. Chem. Soc.* **2004**, *126*, 14734–14735.
(39) Steinberg, I. Z.; Harrington, W. F.; Berger, A.; Sela, M.; Katchalski, E. *J. Am. Chem. Soc.* **1960**, *82*, 5263–5279.
(40) Horng, J. C.; Raines, R. T. *Protein Sci.* **2006**, *15*, 74–83.
(41) Kang, Y. K.; Jhon, J. S.; Park, H. S. *J. Phys. Chem. B* **2006**, *110*, 17645–17655.
(42) Renfrew, P. D.; Butterfoss, G. L.; Kuhlman, B. *Proteins* **2008**, *71*, 1637–1646.
(43) Butterfoss, G. L.; Hermans, J. *Protein Sci.* **2003**, *12*, 2719–2731.

Scheme 3. Peptoids with High-Resolution Structures

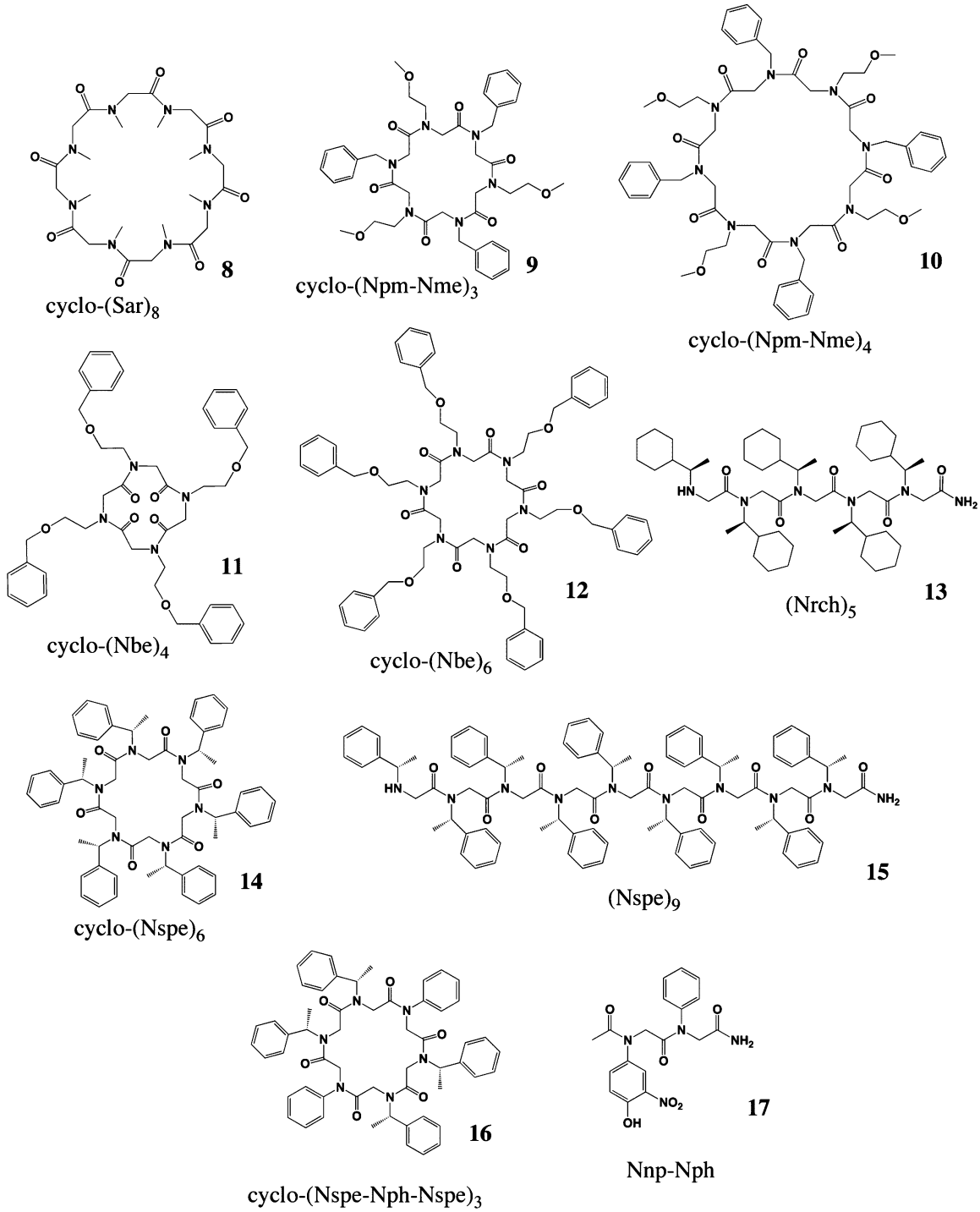

Energy Scans. All quantum calculations were carried out with the Gaussian03 package[44] and used the tight self-consistent field option. We determined Ramachandran-type energy surfaces of the disarcosine model (molecule **1**) by combinatorialy fixing ψ_{i-1}, ϕ_i, and ψ_i (Scheme 1) at every 15° from −180° to 180°.[19] Conformations were minimized at the HF/6-31G* level and single point energies calculated at the B3LYP/6-31G* level (see Supporting Information for MP2(full)/6-31G*//HF/6-31G* energies, Figure S2). We ran two screens with ω_i in either a cis or trans conformation. The only constraints during minimization were the three fixed backbone torsions.

Landscapes. We generated the ϕ_i vs ψ_i energy surfaces of molecule **1** (Figure 1) using the following steps: (1) We identified the lowest energy conformation at each (ϕ_i, ψ_i) position from among the 24 structures with different ψ_{i-1} values. (2) We then smoothed the surfaces slightly by averaging the energies of all structures at each (ϕ_i, ψ_i) that were within 0.6 kcal/mol of the lowest energy conformation for each particular dihedral angle pair. (3) We forced center symmetry in the plot by assigning the lowest energy from either symmetric pair of points (ϕ_i, ψ_i), ($-\phi_i$, $-\psi_i$) to both. This last step was performed to account for the fact that ϕ_{i-1} was not explicitly screened and may have been caught in higher energy local minima in one component of the pair, (slightly influencing the overall energy) as well as other small differences that may have

(44) Frisch, M. J.; et al. *Gaussian*, revision E.01; Gaussian, Inc.: Wallingford, CT, 2004.

arisen during minimization. (The unsmoothed and unsymmetrized contours are provided in the Supporting Information, Figure S1.)

We generated the ψ_i vs ω_i and ϕ_i vs ω_i energy surfaces of molecule **1** (Figure 4) by binning structures generated in the above screens in 10° ω_i windows (ω_i was not fixed during minimizations). The plots were also smoothed and symmetrized as above.

We determined ϕ_i vs ψ_i energy surfaces of molecules **5** and **6** (Figure 6) by scanning ϕ and ψ every 15° from −180° to 165° (for both cis and trans ω conformations) at the B3LYP/6-311+G(2d,p)//HF/6-31G* level. The smaller number of structures to be scanned allowed for the use of a larger basis set, which we also used for the rest of the calculations described below. The plots are shown from 0° to 360°, thus the data from points with ϕ or ψ = 0° are repeated at ϕ or ψ = 360°. The plot for the achiral molecule **5** was symmetrized as above for Figure 1; this accounted for differences in energy between pairs of structures with center-symmetric backbone torsions but asymmetric side chain torsions, as each structure was minimized from a starting conformation with χ_1 approximately −90°. Two scans were run for molecule **6**, with the χ_1 torsion starting at either a positive or negative value. The energy surface was generated by selecting the lowest energy at each (ϕ, ψ) position from the two rotamers.

***ω* Angles.** We used N,N-dimethylacetamide (molecule **2**) as a model for the peptoid ω torsion by fixing a C−C−N−C torsion at particular angle and calculating energies at the B3LYP/6-311+G(2d,p)//HF/6-31G* level. The N-dimethyl group does not rotate as a rigid body, and thus each minimized structure has two ω angles. We calculated the lowest energy path around omega by measuring both C−C−N−C torsions for the set of optimized structures and taking the lowest energies within local ω windows. We transformed energy into probability (Figure 3) using the Boltzmann equation assuming a temperature of 300 K.

***χ* Angles.** We generated the χ_1 torsional potentials for molecules **3** and **4** (Figure 5) at the B3LYP/6-311+G(2d,p)//HF/6-31G* level of theory by fixing backbone at cis α_D (ϕ, ψ) = (−90°, 180°) trans α_D (−90°, 180°) and trans $C_{7\beta}$ (−130°, 80°) and rotating around χ_1. The experimental data in Figure 5A were converted to (−ϕ, −ψ) if $\phi > 0°$. The experimental data for the β-branched set (Figure 5B) were not adjusted in this manner due to chirality considerations.

Table 2. Torsions of Favorable Conformations for Molecule **1**[a]

conformation	ω_i	ϕ_i	ψ_i
cis α_D	−15.59°	−83.42°	−168.46°
trans α_D	171.87°	−79.91°	175.89°
trans $C_{7\beta}$	179.03°	125.51°	−71.25°

[a] Values represent one of two centro-symmetric isoenergetic minima.

Acknowledgment. We thank Frances Bauer and Joseph Hargitai of NYU IT services for technical assistance. We thank Barney Yoo and Consiglia Tedesco for providing structures. R.B. and G.B. are supported by National Science foundation DBI 0820757. K.K. is supported by a National Science foundation CAREER Award (CHE-0645361).

Supporting Information Available: Tables of torsions in experimental peptoid structures; nonaveraged and nonsymmetrized Ramachandran-type energy landscapes for molecule **1**; MP2 energy landscapes for molecule **1**; minimization of peotoid in a $C_{7\beta}$ with a aryl side chain at i+1; minimized structures of molecule **1**; analysis of the energies of the stationary points; description and analysis of peptoid amide bond twist and pymiridalization;[34] and the complete ref 44. This material is available free of charge via the Internet at http://pubs.acs.org.

JA905267K